

The origin of the stabilized simple-cubic structure in polonium

B. I. Min¹, J. H. Shim¹, Min Sik Park¹, Kyoo Kim¹, S. K. Kwon¹, and S. J. Youn²
¹*Department of Physics, Pohang University of Science and Technology, Pohang 790-784, Korea*
²*Department of Physics Education, Gyeongsang National University, Jinju 660-701, Korea*
 (Dated: November 19, 2018)

The origin of the stabilized simple-cubic (SC) structure in Po is explored by using the first principle band calculations. We have found that the prime origin is the inherent strong spin-orbit (SO) interaction in Po, which suppresses the Peierls-like structural instability as usually occurs in p -bonded systems. Based on the systematic analysis of electronic structures, charge densities, Fermi surfaces, and susceptibilities of Se, Te, and Po, we have proved that the stable crystal structure in VIA elements is determined by the competition between the SO splitting and the crystal field splitting induced by the low-symmetry structural transition. The trigonal structure is stabilized in Se and Te by the larger crystal field splitting than the SO splitting, whereas in Po the SC structure is stabilized by the large SO splitting.

PACS numbers: 61.66.Bi, 71.70.Ej, 71.20.Gj

Among the elements in the periodic table, only Po (polonium) is known to crystallize in the simple-cubic (SC) structure in nature¹. Radioactive Po, which was discovered by Pierre and Marie Curie in 1898, requires difficult sample preparation, and so not many experimental and theoretical studies have been carried out. Po, which is located in the VIA column of the periodic table, has a valence electron configuration of $6s^26p^4$ ($Z=84$), and exhibits two metallic phases of α and β which are formed in the SC and the rhombohedral (trigonal) structure below and above $\sim 348K$, respectively^{2,3}. Note that the isoelectronic elements located in the same VIA column, Se (selenium) and Te (tellurium), crystallize in the trigonal structure (space group $P3_121$) with the helical chain arrangements of atoms, which run parallel to the crystallographic c axis of the hexagonal setting. Hence the coordination number is two in trigonal Se and Te in contrast to six in simple-cubic Po (SC-Po). The ratio of the intrachain (d_1) bond length to the interchain (d_2) bond length is $\frac{d_2}{d_1} = 1.50, 1.23, \text{ and } 1.0$ for Se, Te, and Po, respectively. The coordination number of two in trigonal Se and Te can be understood based on the simple octet rule⁴.

The reason why metallic Po has a stable SC structure has not been fully addressed yet. By using the relativistic parameterized extended Hückel method, Lohr⁵ has found a hint that the helical structure as a distortion of a SC structure might be quenched in the case of Po due to its very large spin-orbit (SO) coupling. However, their calculation was not self-consistent and adopted the atomic value of the SO coupling parameter. They did not study the structural energetics. Recently, using the *ab-initio* pseudopotential band method, Kraig *et al.*⁶ showed that the SC structure is preferred by Po to face-centered or body-centered cubic structure. They argued that the large s - p splitting in Po would produce the stable SC structure. However, they could not explain why this happens only in Po but not in other elements with similarly large s - p splittings. Moreover, the SO interaction was not taken into account in their band

calculations. Lach-hab *et al.*⁷ studied the structural energetics for Po using the tight-binding (TB) band method. After having determined the TB parameters by fitting the TB bands to the semirelativistic full-potential linearized augmented plane-wave (FLAPW)⁹ bands, they took account of the SO effect *a posteriori* by employing the atomic value of the SO coupling parameter. They found that the SC structure is the most stable among the close-packed structures for both cases with and without the SO effect included. They did not consider the lower symmetry structures with the internal atomic relaxation, as observed in Se and Te.

A systematic crystallographic transformation can occur from the SC lattice to the trigonal lattice. As shown in Fig. 1(a), the SC lattice can be described by a hexagonal lattice in which the hexagonal a axis corresponds to the face diagonal and the hexagonal c axis to the body

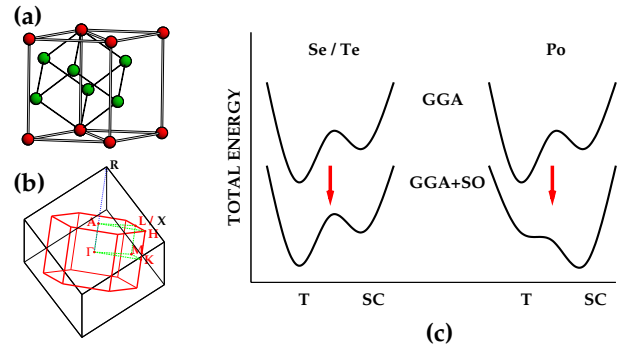


FIG. 1: (a) A hexagonal unit cell with tripled volume of a SC unit cell. (b) The hexagonal Brillouin zone (BZ) compared to the SC BZ. Note that Γ -A and Γ -L in the hexagonal BZ correspond to $\frac{1}{3}\Gamma$ -R and Γ -X in the SC BZ. (c) Schematic total energy curves for Se, Te, and Po in the hypothetical structural space. T and SC represent trigonal and simple-cubic structures, respectively. Both in the GGA and GGA+SO, trigonal Se and Te are more stable. For Po, trigonal Po is more stable in the GGA, while SC-Po becomes more stable in the GGA+SO.

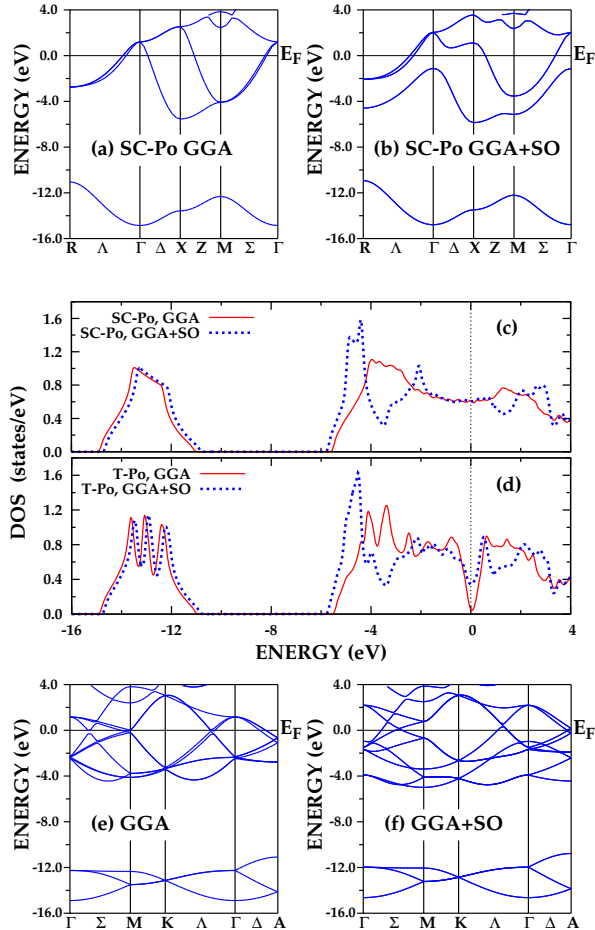


FIG. 2: (a)-(b) The GGA and GGA+SO band structures of SC-Po. (c)-(d) DOSs of SC-Po and trigonal Po. The latter corresponds to the stable phase obtained after the geometry optimization in the GGA scheme. In each frame, DOSs obtained by the GGA and GGA+SO schemes are compared. (e)-(f) The GGA and GGA+SO band structures of SC-Po drawn in the frame of the hexagonal BZ. There are several band crossings at E_F in the GGA, but not in the GGA+SO.

diagonal of cube. Then the size of the unit cell becomes tripled with $c/a = \sqrt{\frac{3}{2}}$. The trigonal structure of β -Po corresponds to the elongated SC structure simply along the body diagonal direction. In the trigonal structures of Se and Te, the internal atomic position parameters are also changed in addition to elongation⁸.

To explore the origin of stabilized SC structure in Po, we have investigated the electronic and structural properties of Se, Te, and Po systematically by using the first-principles FLAPW band method incorporating the SO interaction. For the calculations, the QMD-FLAPW⁹ and the WIEN2K¹⁰ codes are utilized. The band structure results obtained from both codes are qualitatively coincident with each other. Below we will use mainly WIEN2K results, since the local orbital basis is im-

plemented in WIEN2K in order to describe the relativistic $6p_{1/2}$ wave function correctly¹¹. The exchange-correlation interaction is treated by the generalized gradient approximation (GGA)^{12,13}.

We have first studied the structural energetics by optimizing the atomic positions for both trigonal and SC structures of Se, Te, and Po with (GGA+SO) and without (GGA) the SO interaction. In the GGA scheme, the trigonal structures are more stable than SC structures by 0.092, 0.031, and 0.004 eV/atom for Se, Te, and Po, respectively. The GGA+SO scheme, however, yields different results. The incorporation of the SO coupling reduces the stability of the trigonal structure. For Se and Te, the trigonal structure is still more stable than the SC structure by 0.090 and 0.021 eV/atom, respectively. In contrast, for Po, the SC structure becomes more stable than the trigonal structure by 0.016 eV/atom. Thus the total energy behaves as in Fig. 1(c). There are two local minima in the hypothetical structural space, the trigonal (T) and the SC structure. The SO coupling effect does not change the global minima in Se and Te, but changes that in Po from trigonal Po to SC-Po. This finding indicates that the SO interaction plays an essential role in stabilizing the SC structure of Po.

Indeed band structures in Fig. 2(a)-(b) reveal that the effect of the SO interaction is substantial for SC-Po, as compared to that for Se and Te. The lowest bands in Fig. 2(a)-(b) correspond to Po $6s$ states, while the bands near the Fermi level (E_F) to Po $6p$ states. Due to the large energy gap between $6s$ and $6p$ states, there will not be a considerable mixing between them, and thus Po can be classified as a p -bonded system. When the SO interaction is taken into account, the degenerate $6p$ bands along Γ -X, Γ -M, and Γ -R are split so that the doubly degenerate $6p_{1/2}$ band is separated from the upper half-filled $6p_{3/2}$ band. Due to the SO splitting, the small hole Fermi surface at Γ disappears. The SO splitting of p states at Γ for SC-Po is as much as 3.16 eV, which is much larger than those for SC structures of Se and Te, 0.53 and 1.05 eV.

In Fig. 2(c)-(d), we have compared the density of states (DOS) of SC-Po and that of trigonal Po, which are obtained by the GGA and GGA+SO schemes. Trigonal Po here corresponds to the stable phase determined by the geometry optimization in the GGA scheme. Notable in the GGA-DOS is the pseudogap feature at E_F for trigonal Po, which would give rise to the semi-metallic behavior. The pseudogap appears between the nonbonding lone-pair and the antibonding Po $6p$ state, because of the splitting between the bonding and antibonding Po $6p$ state in the chain arrangement of trigonal Po¹⁴. Hence the DOS at E_F , $N(E_F)$, becomes much reduced in trigonal Po from that in SC-Po. In fact, the stable trigonal phases of Se and Te result from this gap formation near E_F . In the case of Se, the energy splitting between the bonding and the antibonding state is so large that the system becomes insulating, while Te is semimetallic.

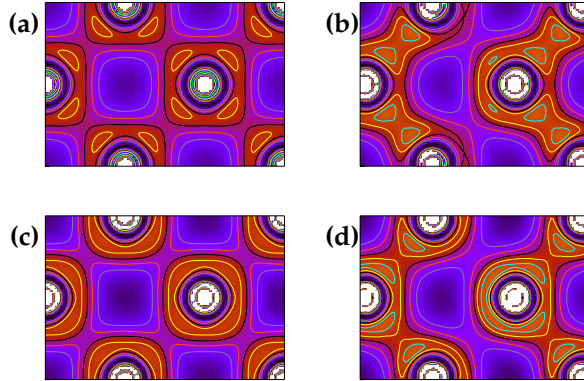


FIG. 3: The occupied charge density distributions of Po $6p$ bonding states in the energy range of $-6.0 \sim -3.0$ eV. (a) SC-Po (GGA), (b) trigonal Po (GGA), (c) SC-Po (GGA+SO), and (d) trigonal Po (GGA+SO).

In the GGA+SO scheme, the $6p_{1/2}$ state is separated out, and so the band shape and $N(E_F)$ are changed a lot. Occupied band widths are broadened with more weight at low energy side, which produces energy gains for both SC-Po and trigonal Po. The stable SC-Po in the GGA+SO scheme reflects that the SO induced energy gain is larger for SC-Po than for trigonal Po. It is because $N(E_F)$ for trigonal Po is rather enhanced producing some energy loss. Note that, for Se and Te, both the GGA and GGA+SO schemes yield similar DOS, implying no noticeable energy gain from the SO interaction. These results suggest that the stable crystal structure in VIA elements is mainly determined by the competition between the SO splitting and the crystal field splitting due to the low symmetry structure. That is, for Se and Te, the larger crystal field splitting between the intrachain bonding and antibonding states stabilizes the trigonal structure, whereas, for Po, the larger SO splitting stabilizes the SC structure.

The stable trigonal structure of Se and Te can be understood in terms of the three dimensional (3D) Peierls distortion of the SC structure^{4,8,15}. In general, p -bonded systems would favor the SC structure to maximize the directional p_σ bonding. However, three mutually orthogonal linear chains in the SC structure will be easily distorted by the Peierls mechanism when the linear chain is partially filled. In the case of Se and Te, each chain is $2/3$ -filled, and so the energy gain can be achieved by the trimerization with the short-long-long bond alternation. Decker *et al.*¹⁶ recently demonstrated this mechanism for Te by comparing the band structures of the undistorted SC and the distorted trigonal structure. The structural distortion from the SC to the trigonal structure induces a splitting of degenerate bands near E_F , which yields the energy gain for trigonal Te.

We have examined the above scenario for SC-Po. Fig-

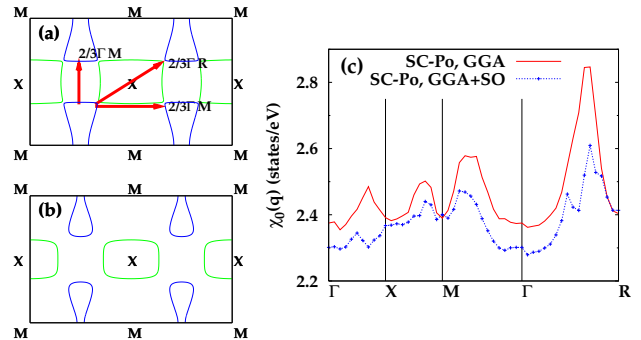


FIG. 4: Fermi surfaces of SC-Po derived from the third (green) and fourth (blue) bands in the GGA (a) and the GGA+SO (b). (c) Susceptibilities of SC-Po in the GGA and the GGA+SO.

ure 2(e)-(f) display the GGA and GGA+SO band structures of undistorted SC-Po which are projected in the hexagonal BZ. The GGA band of Fig. 2(e) shows several band crossings at E_F which are created by the back-folding of bands of the larger SC BZ into the smaller hexagonal BZ (see Fig. 1(b)). Then, as in Te¹⁶, a Peierls-like structural distortion would split the band crossings at E_F to yield the energy gain. In contrast, the GGA+SO band of Fig. 2(f) shows the band crossings not at E_F but at higher or lower energy side far apart from E_F . This is because of the substantial band shift by the SO splitting. Accordingly, no energy gain would result from the Peierls-like structural distortion. This proves how the SO interaction stabilizes the SC structure of Po. When Decker *et al.*¹⁶ demonstrated this mechanism for Te, they did not take into account the SO interaction. The SO induced band shift in Te, however, is not large enough to suppress the Peierls-like instability.

The bonding characters can be investigated by the charge density plot. Figure 3 shows the occupied charge density distributions of Po $6p$ bonding states in the energy range of $-6.0 \sim -3.0$ eV for both SC-Po and trigonal Po. They are plotted on the special plane of hexagonal unit cell to see the bonding character along the helical zig-zag chains in the c -direction. The GGA charge density for SC-Po (Fig. 3(a)) shows larger bonding character between Po atoms than the GGA+SO charge density (Fig. 3(c)). This implies that the directional bonding between atoms becomes weakened when incorporating the SO interaction, and so the charge density becomes more isotropic. This feature is more clearly seen in trigonal Po which manifests the prominent chain nature. The GGA charge density for trigonal Po (Fig. 3(b)) shows a pronounced intrachain bonding character along the zig-zag chains. In the GGA+SO charge density (Fig. 3(d)), the SO interaction weakens the intrachain directional bondings so that the anisotropic chain nature is suppressed. This is consistent with the enhanced $N(E_F)$ in the GGA+SO DOS in Fig. 2(d). The charge density

plots reveal that the SO interaction weakens the directional bondings between Po atoms and so suppresses the 1D chain nature and the corresponding Peierls-like structural instability.

The structural transition can also be studied by analyzing the behavior of the charge susceptibility $\chi_0(q)$. $\chi_0(q)$'s in Fig. 4(c) are obtained from the band structures of SC-Po. $\chi_0(q)$ in the GGA scheme shows the highest peak near $\vec{Q} = \frac{2}{3}\Gamma$ -R, indicating a possible structural instability at this \vec{Q} . This \vec{Q} vector is coincident with the reciprocal lattice vector connecting the hexagonal BZ boundaries including A (see Fig. 1(b)), at which the bands of SC-Po along Γ -R are folded back. Therefore, this peak is closely related to the trigonal distortion of the SC structure along the (111) direction. Noteworthy in Fig. 4(c) is the substantial reduction of this peak of $\chi_0(q)$ when incorporating the SO interaction. The absence of the structural instability in Po would be closely correlated to this behavior of $\chi_0(q)$. One can also note the peaks in $\chi_0(q)$ near $\vec{q} = \frac{2}{3}\Gamma$ -X, $\frac{2}{3}\Gamma$ -M, $\frac{2}{3}\Gamma$ -M. These peaks and the peak near \vec{Q} are expected to arise from the quasi-1D Fermi surfaces of SC-Po, which are formed by the third and fourth bands in Fig. 2(a). Namely, each \vec{q} producing the peak in $\chi_0(q)$ corresponds to the nesting vector of the quasi-1D Fermi surfaces projected in each symmetry plane. The GGA Fermi surfaces in Fig. 4(a), which are drawn in the (220) plane of the SC BZ, exhibit the clear quasi-1D nature with the corresponding nesting vectors. As shown in Fig. 4(b), the SO interaction breaks these quasi-1D Fermi surfaces into pieces, and so reduces the nesting effect. This situation in Po is different from that in Se and Te, in which the 1D nature is preserved

even with the SO interaction, so that the nesting effect is still active.

Finally, it is worthwhile to discuss the stable structures of neighboring elements of Po, Bi ($Z=83$) and At ($Z=85$), both of which are also p -bonded metallic systems with the large SO interaction. In nature, Bi crystallizes in the trigonal (α -arsenic) structure¹⁷. As for radioactive At, no structural information is available because of its too short half-life of only 8.3 hours. α -arsenic structure of Bi can be understood as arising from the Peierls-like distortion, as discussed above^{4,15}. Since the $6p$ -bands in Bi are half-filled, the tendency of the Peierls instability is predominating so as to drive the structural distortion despite the large SO interaction. In the case of At, the $6p$ -bands are 5/6-filled so that the SO interaction would dominate over the Peierls instability as in Po. Hence the SC structure is expected to be stabilized for At.

In conclusion, we have clarified that the origin of the stabilized SC structure in Po is its inherent strong SO interaction. The large SO interaction in Po weakens the directional bondings between atoms so as to suppress the Peierls-like distortion. Our study also reveals that the stable crystal structure in VIA elements is determined by the competition between the SO splitting and the crystal field splitting induced by the structural transition to a lower symmetry. For Se and Te, the larger crystal field splitting between the intra-chain bonding and the anti-bonding state stabilizes the trigonal structure, whereas, for Po, the larger SO splitting stabilizes the SC structure.

This work was supported by the SRC program of MOST/KOSEF and in part by the KRF.

-
- ¹ W. H. Beamer and C. R. Maxwell, J. Chem. Phys. **14**, 569 (1946).
² C. R. Maxwell, J. Chem. Phys. **17**, 1288 (1949).
³ R. J. Desando and R. C. Lange, J. Inorg. Nucl. Chem. **28**, 1837 (1966).
⁴ J.-P. Gaspard, A. Pellegatti, F. Marinelli, C. Bichara C, Phil. Mag. B **77**, 727 (1998).
⁵ L. L. Lohr, Inorg. Chem. **26**, 2005 (1987).
⁶ R. E. Kraig, D. Roundy, and M. L. Cohen, Solid State Comm. **129**, 411 (2004).
⁷ M. Lach-hab, B. Akdim, D.A. Papaconstantopoulos, M.J. Mehl, N. Bernstein, J. Phys. Chem. Solid **65**, 1837 (2004).
⁸ G. Kresse, J. Furthmuller, and J. Hafner, Phys. Rev. B **50**, 13181 (1994).
⁹ E. Wimmer, H. Krakauer, M. Weinert, and A. J. Freeman, Phys. Rev. B **24**, 864 (1981); M. Weinert, E. Wimmer, and A. J. Freeman, *ibid.* **26**, 4571(1982); H. J. F. Jansen and A. J. Freeman *ibid.* **30**, 561 (1984).
¹⁰ P. Blaha, K. Schwarz, G. K. H. Madsen, K. Kvasnicka, and J. Luitz, WIEN2K (Karlheinz Schwarz, Technische Universität Wien, Austria, 2001).
¹¹ D. Singh, Plane waves, Pseudopotentials, and the LAPW Method (Kluwer Academic, Boston, 1994).
¹² J.P. Perdew and Y. Wang, Phys. Rev. B **45**, 13244 (1992).
¹³ We have found that the GGA describes the ground states of Se, Te, and Po better than the LDA.
¹⁴ J. D. Joannopoulos, M. Schlüter, and M. L. Cohen, Phys. Rev. B **11**, 2186 (1975).
¹⁵ J. K. Burdett and S. Lee, J. Amer. Chem. Soc., **105**, 1079 (1983).
¹⁶ A. Decker, G. A. Landrum, and R. Dronskowski, Z. Anorg. Allg. Chem., **628**, 295 (2002).
¹⁷ A. B. Shick, J. B. Ketterson, D. L. Novikov, and A. J. Freeman, Phys. Rev. B **60**, 15484 (1999).